Surface Plasmon Resonance

DOI: 10.1002/ange.200905805

Plasmonic Modulation of the Upconversion Fluorescence in $NaYF_4$:Yb/Tm Hexaplate Nanocrystals Using Gold Nanoparticles or Nanoshells**

Hua Zhang, Yujing Li, Ivan A. Ivanov, Yongquan Qu, Yu Huang, and Xiangfeng Duan**

The ability to tune the spectral properties of rare-earth-element-doped upconversion nanocrystals (NCs), which can emit light at shorter wavelengths than the excitation source, is of considerable interest for biomedical imaging and therapeutics.[1–5] Nanoscale integration of multiple functional components can enable exciting new opportunities to precisely control and fine-tune the electronic and optical properties of the resulting materials. Herein we report a new approach to modulate upconversion emission through hetero-integration of the upconversion NCs with plasmonic gold nanostructures. Our studies show that gold nanoparticles (NPs) can be attached with variable density onto the upconversion NCs, which can then function as the nucleation seeds for the growth of continuous gold nanoshells. The attachment of gold NPs has been found to greatly enhance the upconversion emission. Spectroscopic studies show that this enhancement has a strong spectral dependence, with a significantly larger enhancement factor near the plasmon-resonance frequency, thus suggesting that the surface-plasmon-coupled emission plays an important role in the enhancement of upconversion emission. On the contrary, gold nanoshells can greatly suppress the NC emission, possibly because of the strong scattering of excitation irradiation. These findings open a new pathway to rationally modulate the upconversion emission, and can broadly impact areas such as biomedical imaging, sensing, and therapeutics, as well as enable new opportunities for energy harvesting and conversion.

Surface plasmon resonance (SPR) is the collective electron-cloud oscillation on a metal surface or NP, and is caused by the interaction of the metal with incident light.[6,7] This interaction leads to a number of interesting optical events such as the absorption and scattering of photons of certain wavelength, and is responsible for the wide range of colors observed in metal nanoparticle colloids.[8,9] Additionally, the large local electric fields generated by SPR in the vicinity of the NPs can significantly modify the spectroscopic properties of neighboring fluorophores.[10–12] SPR is largely responsible for surface-enhanced Raman spectroscopic (SERS) effects, with an enhancement factor of up to 10^{14}–10^{15}, thus allowing the technique to be sensitive enough for single-molecule detection.[13–15] Recently, gold and silver NPs, or "islands", have been explored to modulate fluorescent emission from various nanostructures such as semiconductor quantum dots or fluorescent molecules.[16–18]

Our $NaYF_4$:Yb/Tm NCs were synthesized by thermal decomposition of rare-earth/sodium trifluoroacetate precursors in oleic acid and octadecene.[19] The as-synthesized NCs are terminated with oleic acid ligands, and have a hydrophobic character. The attachment of gold NPs and the growth of gold nanoshells are typically carried out in aqueous solution, therefore requiring the dispersion of the NCs in water. To this end, two surface-modification steps have been performed for gold seed attachment and gold shell growth (Figure 1; also see the Supporting Information). Firstly, a ligand-exchange process was carried out by using poly(acrylic acid) (PAA) as a multidentate ligand that displaces the original hydrophobic ligands on the NC surface. The resulting PAA-coated NCs are typically negatively charged. To facilitate the subsequent attachment of the negatively charged gold NPs, an additional layer of poly(allylamine hydrochloride) (PAH) was coated onto the NC surface to render them positively charged. To ensure that each surface-modification process was successful, FTIR spectra were recorded to confirm the additional existence of the -COOH or -NH_2

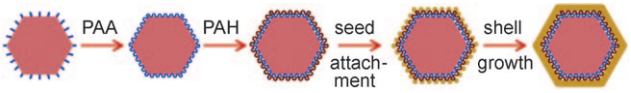

Figure 1. Illustration of surface functionalization, gold NP attachment, and gold nanoshell growth on the upconversion NCs.

[*] H. Zhang, Y. Li, Prof. Y. Huang
Department of Materials Science and Engineering
University of California, Los Angeles, CA 90095 (USA)
E-mail: yhuang@seas.ucla.edu
I. A. Ivanov, Dr. Y. Qu, Prof. X. Duan
Department of Chemistry and Biochemistry
University of California, Los Angeles, CA 90095 (USA)
E-mail: xduan@chem.ucla.edu
Prof. Y. Huang, Prof. X. Duan
California Nanosystems Institute
University of California, Los Angeles, CA 90095 (USA)

[**] X.D. acknowledges partial support by the NIH Director's New Innovator Award Program, part of the NIH Roadmap for Medical Research (grant no. 1DP2OD004342-01). Confocal laser scanning microscopy was performed at the CNSI Advanced Light Microscopy/Spectroscopy Shared Resource Facility at UCLA, supported with funding from an NIH-NCRR shared resources grant (CJX1-443835-WS-29646) and an NSF Major Research Instrumentation grant (CHE-0722519).

Supporting information for this article is available on the WWW under http://dx.doi.org/10.1002/anie.200905805.

groups (see the Supporting Information). To attach the gold NPs onto the NC surface, negatively charged gold NPs were prepared separately and then mixed with the aqueous solution of upconversion NCs in the desired ratio, and allowed to age for a controlled time. Gold shell growth was then carried out by introducing additional gold precursors and reductant into the upconversion NC solution.

The microstructures, morphologies, and composition of the $NaYF_4$:Yb/Tm NCs were characterized by TEM studies. The as-prepared upconversion NCs typically have a hexagonal structure with uniform size of approximately 180 nm (Figure 2a). The relatively uniform contrast in the TEM

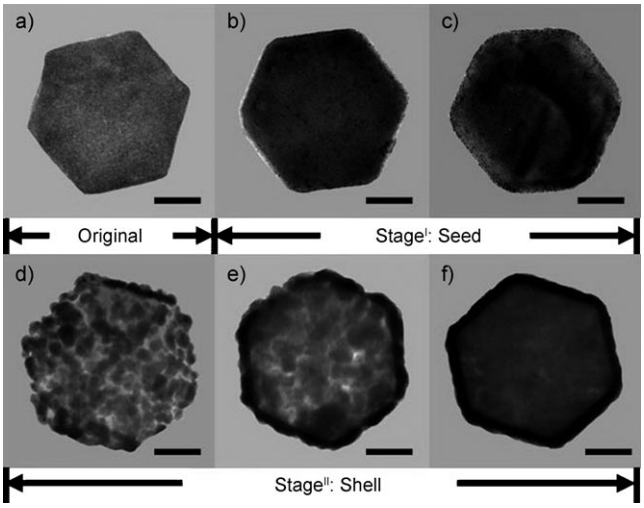

Figure 2. Time-lapse TEM images of the upconversion NCs during the process of gold seed attachment and shell growth, a) original, b–c) with increasing number of attached gold NPs and d–f) with growing gold nanoshells (scale bar: 50 nm).

image suggests the NCs are single crystals, which was confirmed by high-resolution TEM images and electron diffraction patterns (see the Supporting Information). With the attachment of gold NPs, an increasing number of darker specks can be observed; each dark speck corresponds to a gold NP on the NC surface (Figure 2b,c). During the Au shell growth stage, these Au NPs function as the seeds for the nucleation of gold on the NC surface. As the reaction proceeds, the size of the gold NPs grows rather quickly and eventually the NPs merge together to form a continuous shell (Figure 2d–f).

The upconversion emission spectra of the NCs were collected in aqueous solution (ca. 1 wt%) under 980 nm diode laser excitation with a power density of approximately 50 mW cm^{-2}. The emission spectra of the upconversion NCs during the seeding stage show a significant increase in emission intensity as the number of attached Au NPs increased, and an enhancement factor of more than 2.5 was achieved (Figure 3a). On the other hand, during the gold shell growth stage, the evolution of emission spectra show that the emission intensity decreases substantially as the shell forms (Figure 3b). These studies clearly demonstrate that the attachment of gold NPs on the upconversion NC surface

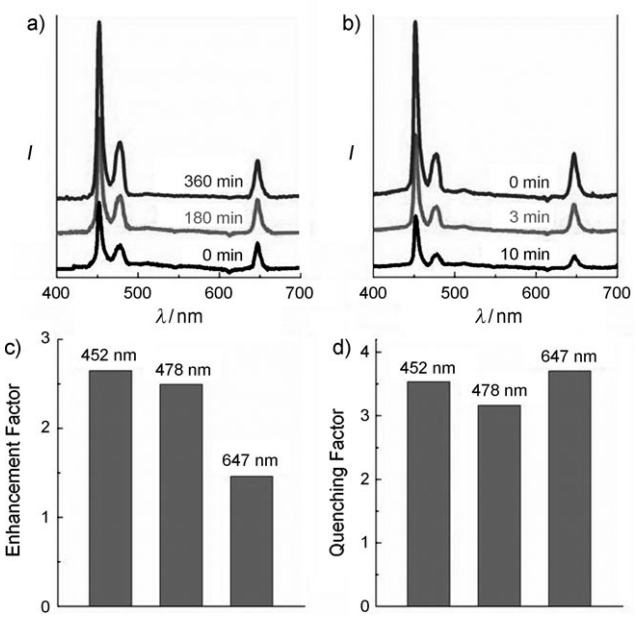

Figure 3. Room-temperature upconversion emission spectra of $NaYF_4$:Yb/Tm NCs during a) gold seed attachment stage (0–360 min) and b) gold shell growth stage (0–10 min). c) Enhancement factors after gold NP attachment and d) quenching factors after gold shell growth at different emission wavelengths.

can enhance the upconversion emission, while the formation of the continuous gold shell can quench the emission. Additionally, it is interesting to note that the emission enhancement by Au NPs is highly wavelength-dependent, as the enhancement factors in the violet/blue region are much larger than those in the red region (Figure 3c). Specifically, more than 150% increase in emission intensity was observed at 452 nm and 476 nm, while an increase of only approximately 50% was seen at 647 nm. On the other hand, the quenching of the emission by the gold shell is far less dependent on the wavelength; the quenching factors remain essentially the same for all emission peaks (Figure 3d).

To confirm that the modulation in emission intensity indeed originates from individual upconversion NCs rather than any other complex effect in solution, we used confocal microscopy to investigate the upconversion emission from individual NCs. To this end, the NCs were first spin-coated onto a glass slide, and then cured in gold seed solution for Au NP attachment, while the upconversion emission was monitored with increasing curing time. To ensure that emission from the same location was compared, we used lithography to create alignment markers on the glass slide. The reflection image of the NCs on the glass slide shows well-separated NCs or NC clusters (Figure 4a). The SEM image of a similar sample prepared on a silicon wafer further shows that the NCs exist as either single NCs or a few NC clusters (Figure 4b). The confocal fluorescence image (Figure 4c–e) of the same sample area shown in Figure 4a clearly shows strong upconversion emission from the NCs when excited with a 980 nm laser, with each bright spot in the image corresponding to emission from one or a few NCs. Importantly, the confocal images clearly show that the upconversion emission from

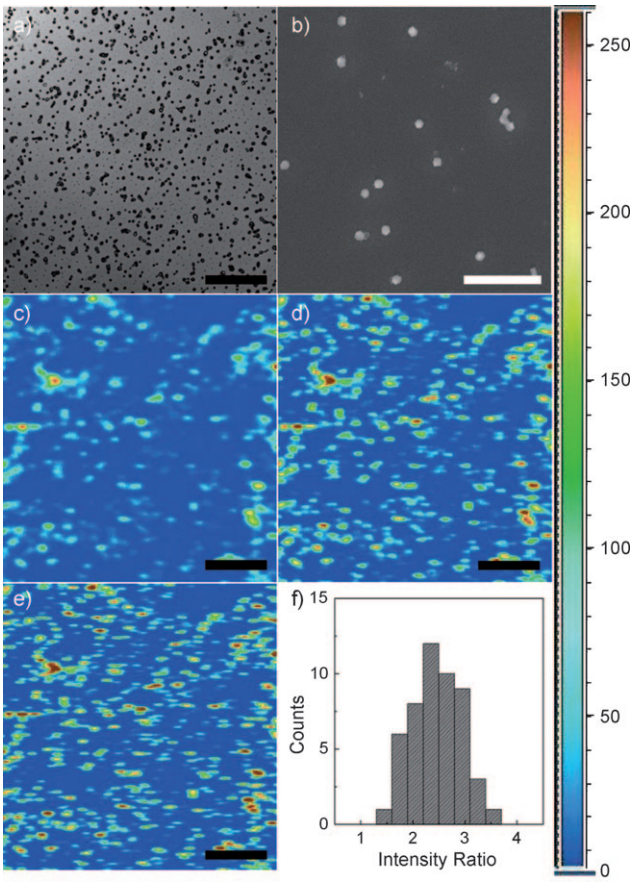

Figure 4. a) Reflection image of NCs on glass substrate. b) SEM image of a similar sample prepared on silicon wafer. Confocal upconversion fluorescence images of the upconversion NCs dipped into gold seed solution for c) 0 min, d) 180 min, and e) 360 min. f) Histogram of the enhancement factors of 50 bright spots (intensity ratio between (e) and (c)). Scale bars: 3 μm (b) and 20 μm (a, c, d, e).

individual NCs can be significantly enhanced with increasing curing time in gold seed solution, thus demonstrating that the enhancement can be attributed to individual NCs with attached gold NPs. Quantitative analysis of the confocal images shows that an intensity enhancement factor of approximately 2.6 can be achieved (Figure 4 f), which is consistent with the results shown in Figure 3 a.

The observed enhancement in the upconversion emission is in stark contrast to the usual perception that the presence of the metal in such proximity can lead to quenching of the fluorescence emission. We suggest the enhancement effect from the gold NPs may be attributed to at least two possible factors: 1) an increase of the excitation rate by local field enhancement (LFE), that is, an enhancement of the effective excitation flux caused by LFE associated with plasmonic resonance; 2) an increase of the emission rate by surface-plasmon-coupled emission (SPCE), that is, an enhancement of emission efficiency because of the coupling of the upconversion emission with the NP plasmonic resonance, which will effectively increase both the nonradiative and radiative decay rate. SPCE can occur when the emission band of the fluorophore overlaps with the plasmon resonance frequency of the metal nanostructures.[16] Importantly, both of these factors have been used to account for the metal-enhanced fluorescence (MEF) in quantum dots or fluorescent molecules.[17,18]

To understand the interplay between the emission in upconversion NCs and the plasmon resonance in Au NPs, we have characterized the plasmon resonance properties of NC–NP conjugates using UV/Vis absorption spectra. Importantly, the UV/Vis spectra of the gold NPs and NC–NP conjugates show a resonance peak around 510 nm (Figure 5 a), which is

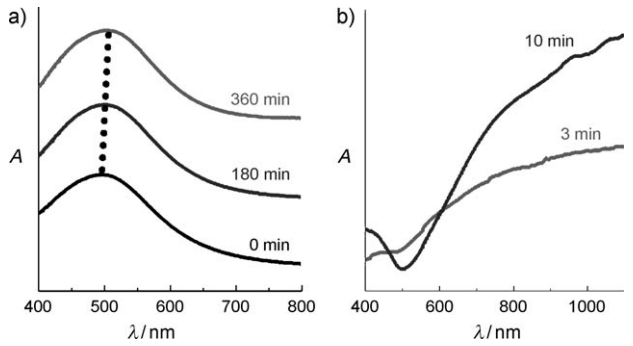

Figure 5. UV/Vis spectra of upconversion NCs a) with gold nanoseeds and b) with gold shells at different times.

consistent with the plasmon resonance frequencies observed in similar gold NPs.[20,21] A slight red shift is observed as the density of gold NPs on the NC surface increases; this observation is also consistent with previous observations that the SPR peak would shift to higher wavelengths with the aggregation of gold NPs.[22–24] This plasmonic resonance frequency of gold NPs overlaps well with the two major emission peaks in the upconversion NCs (452 nm and 478 nm). Therefore, the gold NP SPR can effectively couple with the upconversion emission and can thus increase the radiative decay rate, emission efficiency, and intensity of the NCs. With a better plasmonic coupling near the plasmon resonance frequency, the SPCE is also a reason why the observed enhancement factor is larger for violet/blue emission than for red emission (Figure 3 a, c). These studies suggest that SPCE plays an important role in the spectral dependent enhancement of upconversion emission, although other effects such as LFE may also contribute. On the other hand, when a continuous gold shell was formed, the SPR peak was shifted to the near-infrared region (Figure 5 b). This shift is highly dependent on the thickness and geometry of the gold shell,[25–27] reduces the SPCE, and also significantly increases the scattering of excitation light at 980 nm. Thus, the effective excitation flux is reduced, which leads to a quench of the upconversion emission. Additionally, the complete surrounding gold shell can also block the emission transmittance from the upconversion NCs.

To further study the SPCE effect in our upconversion NC–NP conjugates, we used the time-correlated single photon counting (TCSPC) technique to characterize their fluorescence lifetimes (Figure 6). The lifetime measurement clearly shows that the fluorescence decay of the upconversion NCs

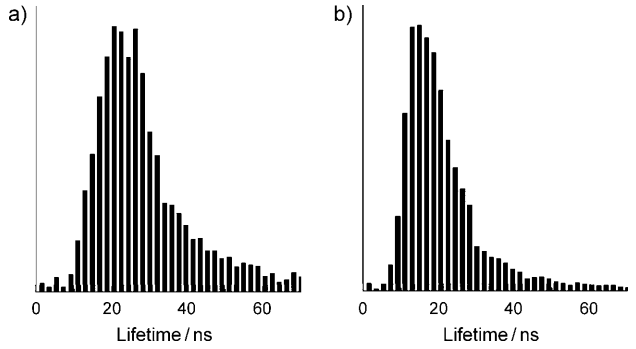

Figure 6. Histograms of lifetimes of a) upconversion NCs and b) upconversion NCs with attached gold NPs.

with gold NPs (average lifetime ca. 21 ns, Figure 6b) is faster than that of the upconversion NCs only (average lifetime ca. 28 ns, Figure 6a). Additionally, it is interesting to note that the lifetime distribution is narrower for NC–NP conjugates than NCs only. However, the exact reason for this change needs further investigation in future studies. This study confirms that the fluorescence decay rates are enhanced by the presence of gold NPs, thus supporting the argument that SPCE can lead to a faster radiative decay rate and enhanced emission efficiency and intensity.

In summary, we have reported a new approach for the modulation of upconversion emission through plasmonic interactions between the upconversion NCs and gold nanostructures. The attachment of the gold NPs onto upconversion NCs can more than double the upconversion emission intensity. This enhancement can be at least partly attributed to SPCE, which can increase the radiative decay rate and emission efficiency, although further study will be necessary to fully elucidate the exact underlying mechanism. The formation of a gold shell can significantly suppress the emission because of considerable scattering of excitation irradiation. These findings open a general pathway to rationally modulate the upconversion emission and applicable in areas including biomedical imaging, therapeutics, and energy conversion.

Received: October 16, 2009
Revised: February 10, 2010
Published online: March 16, 2010

Keywords: fluorescence · nanoparticles · rare earth metals · surface plasmon resonance · upconversion

[1] L. Wang, R. X. Yan, Z. Y. Huo, L. Wang, J. H. Zeng, J. Bao, X. Wang, Q. Peng, Y. D. Li, *Angew. Chem.* **2005**, *117*, 6208; *Angew. Chem. Int. Ed.* **2005**, *44*, 6054.
[2] F. V. D. van de Rijke, H. Zijlmans, S. Li, T. Vail, A. K. Raap, R. S. Niedbala, H. J. Tanke, *Nat. Biotechnol.* **2001**, *19*, 273.
[3] J. Hampl, M. Hall, N. A. Mufti, Y. M. Yao, D. B. MacQueen, W. H. Wright, D. E. Cooper, *Anal. Biochem.* **2001**, *288*, 176.
[4] S. F. Lim, R. Riehn, W. S. Ryu, N. Austin, *Nano. Lett.* **2006**, *6*, 169.
[5] D. Chatterjee, A. J. Rufaihah, Y. Zhang, *Biomaterials* **2008**, *29*, 937.
[6] S. Eustis, M. A. El-Sayed, *Chem. Soc. Rev.* **2006**, *35*, 209.
[7] W. L. Barnes, A. Dereux, T. W. Ebbesen, *Nature* **2003**, *424*, 824.
[8] A. Tao, P. Sinsermsuksakul, P. Yang, *Nat. Nanotechnol.* **2007**, *2*, 435.
[9] M. C. Daniel, D. Astruc, *Chem. Rev.* **2004**, *104*, 293.
[10] F. Le, D. W. Brandl, Y. A. Urzhumov, H. Wang, J. Kundu, N. J. Halas, J. Aizpurua, P. Nordlander, *ACS Nano* **2008**, *2*, 707.
[11] K. G. Thomas, P. V. Kamat, *Acc. Chem. Res.* **2003**, *36*, 888.
[12] J. Zhang, Y. Fu, M. H. Chowdhury, J. R. Lakowicz, *Nano Lett.* **2007**, *7*, 2101.
[13] S. Nie, S. R. Emory, *Science* **1997**, *275*, 1102.
[14] M. A. Mahmoud, M. A. El-Sayed, *Nano Lett.* **2009**, *9*, 3025.
[15] A. Campion, P. Kambhampati, *Chem. Soc. Rev.* **1998**, *27*, 241.
[16] J. R. Lakowicz, *Plasmonics* **2006**, *1*, 5.
[17] I. Gryczynski, J. Malicka, Y. B. Shen, Z. Gryczynski, J. R. Lakowicz, *J. Phys. Chem. B* **2002**, *106*, 2191.
[18] J. R. Lakowicz, *Anal. Biochem.* **2001**, *298*, 1.
[19] J. C. Boyer, L. A. Cuccia, J. A. Capobianco, *Nano Lett.* **2007**, *7*, 847.
[20] S. Link, M. A. El-Sayed, *J. Phys. Chem. B* **1999**, *103*, 4212.
[21] B. J. Messinger, K. Ulrich von Raben, R. K. Chang, P. W. Barber, *Phys. Rev. B* **1981**, *24*, 649.
[22] S. K. Eah, H. M. Jaeger, N. F. Scherer, X. M. Lin, G. P. Wiederrecht, *Chem. Phys. Lett.* **2004**, *386*, 390.
[23] M. J. Feldstein, C. D. Keating, Y. Liau, M. J. Natan, N. F. Scherer, *J. Am. Chem. Soc.* **1997**, *119*, 6638.
[24] J. W. Bai, S. X. Huang, L. Y. Wang, Y. Chen, Y. Huang, *J. Mater. Chem.* **2009**, *19*, 921.
[25] S. J. Oldenburg, R. D. Averitt, S. L. Westcott, N. J. Halas, *Chem. Phys. Lett.* **1998**, *288*, 243.
[26] H. Wang, G. P. Goodrich, F. Tam, C. Oubre, P. Nordlander, N. J. Halas, *J. Phys. Chem. B* **2005**, *109*, 11083.
[27] L. Y. Wang, J. W. Bai, Y. J. Li, Y. Huang, *Angew. Chem.* **2008**, *120*, 2473; *Angew. Chem. Int. Ed.* **2008**, *47*, 2439.